I&EC research
Industrial & Engineering Chemistry Research

Article

pubs.acs.org/IECR

Kinetic Evaluation of the Set of Reactions in the Selective Hydrogenation of 1-Butyne and 1,3-Butadiene in Presence of *n*-Butenes

Javier A. Alves,*[,†,‡] Sergio P. Bressa,[†,‡] Osvaldo M. Martínez,[†,‡] and Guillermo F. Barreto[†,‡]

[†]PROIRQ, Área Departamental Ingeniería Química, Facultad de Ingeniería, The National University of La Plata (UNLP), CP 1900 La Plata, Argentina

[‡]Centro de Investigación y Desarrollo en Ciencias Aplicadas "Dr. J. J. Ronco" (CINDECA), CCT-La Plata-CONICET - The National University of La Plata (UNLP), calle 47 No. 257, CP 1900 La Plata, Argentina

ABSTRACT: The selective hydrogenation in the liquid phase of 1-butyne and 1,3-butadiene in the presence of *n*-butenes over a commercial Pd/Al_2O_3 egg-shell catalyst has been studied. Although hydrogenation of the *n*-butenes and their isomerization are normally undesirable, kinetics of these reactions should also be evaluated in order to carry out the process at efficient operating conditions. Here, the effect of temperature, in the range 25−65 °C, on the specific rate coefficients of 1,3-butadiene hydrogenation reactions and 1-butene, *cis*-2-butene, and *trans*-2-butene hydrogenation and isomerization reactions was evaluated from measurements in a batch reactor system. Further experiments were conducted for the evaluation of selectivity between 1-butyne and 1,3-butadiene hydrogenations at 44 °C. The present results and previous kinetic characterization allow evaluating the most relevant parameters of a set of kinetic expressions for the 10 overall reactions that govern the system transformation.

INTRODUCTION

Catalytic refining of C_4 olefin-rich cuts is carried out by selective hydrogenation of 1,3-butadiene (BD) and acetylenic compounds, typically 1-butyne (BY), on Al_2O_3-supported Pd catalysts.[1] Removal of the highly unsaturated impurities by separation processes, e.g. distillation, is not economically attractive because of similar volatilities of all species in the mixture.

Selective hydrogenation is industrially employed in different applications, such as the preparation of high-purity 1-butene (1BE), mainly used as a copolymer in high-density polyethylene production. This is one of the most stringent processes as regards selectivity, because 1BE should be prevented from hydrogenation to *n*-butane (BA) or isomerization to the more thermodynamically favored isomers, *cis*-2-butene (cBE) and *trans*-2-butene (tBE). In other applications, for example the purification of *n*-olefins for polybutene production, isomerization is not a significant issue. Here we will mainly focus on 1BE purification.

Current technologies employ catalytic fixed beds with cocurrent flow—either down or upflow—of the liquid hydrocarbon mixture and hydrogen.[1] Operating temperatures range from ambient temperature up to around 60−70 °C (e.g., Derrien[1]) and total pressure is raised up to about 10 atm for maintaining the hydrocarbon stream in liquid phase and allowing the desired level of hydrogen partial pressure. BD and BY concentrations in the raw stream usually reach around 1 mole%. The target of selective hydrogenation for 1BE purification is to reduce the amount of impurities to about 5−10 ppm, with minimal losses of 1BE.

Pd has been found as the most effective agent for selective hydrogenation of dienes and acetylenics at relatively low temperatures.[2,3] The selectivity on Pd arises because this metal shows preferential adsorption for hydrocarbons with conjugate or triple bonds. In the present case, the adsorption strength varies as BY > BD ≫ *n*-butenes.[4] Therefore, even small amounts of BY and BD suffice to saturate the active centers, avoiding the adsorption and consequent reactions of *n*-butenes. In practice, however, the catalyst formulation usually includes a second metal (Sn, Ag, Au, Pb, and Zn are some examples) with the purposes of improving selectivity and accelerating the rate of BY hydrogenation. The effect is explained (e.g., Coq and Figueras[5]) by a decrease in the strength of Pd to adsorb the unsaturated species, caused by electronic modification of the co-metal upon Pd. While current commercial catalysts show highly desirable features for eliminating BD and BY at low temperatures, very low concentrations of these compounds immediately lead to the hydrogenation of *n*-butenes and hydroisomerization of 1BE. Therefore, in order to evaluate the performance of a given catalyst, it is necessary to identify the kinetic behavior of all possible reactions in the system.

Although many studies on selective hydrogenation on Pd have been reported in the bibliography, most of them focused on qualitative aspects. As such, the effect of catalyst structure (e.g., metallic particle size) and composition (e.g., the presence and type of promoters), identification of product distribution, reaction mechanisms and intermediates, catalyst deactivation, as caused by oligomer formation on the catalytic surfaces,[6] can be mentioned. The development of kinetic expressions and parameter estimation have been scarcely undertaken, and in most instances the range of experimental conditions was not wide enough for the purpose of simulating or sizing industrial reactors.

Received: October 23, 2012
Revised: February 21, 2013
Accepted: March 25, 2013
Published: March 25, 2013

dx.doi.org/10.1021/ie3029027 | *Ind. Eng. Chem. Res.* 2013, 52, 5849−5861

Schäfer et al.[7] performed kinetic evaluations in both gas and liquid phases, on an egg-shell catalyst of Pd/Al_2O_3. For mixtures containing BY and BD, the dependence of the reaction rates on the hydrocarbon and hydrogen concentrations was analyzed, but values of kinetic parameters were not reported.

In the work of Boitiaux et al.,[8] pressure and temperature levels in the range of industrial practice were employed to describe the main kinetic features of the reaction system. Ratios between kinetic parameters were reported, but not individual values.

Conditions in the range of industrial operations were also explored by Seth et al.[9] for their study of liquid-phase hydrogenation on a laboratory-prepared $Pd/\alpha Al_2O_3$ catalyst. The study focused on the hydrogenation of BD in the presence of isobutylene, a purification step for subsequent dimerization of isobutylene. Simplified Langmuir−Hinshelwood kinetic expressions were employed for fitting the experimental data. An experimental correction factor was introduced to account for the hydrogenation rate of isobutylene in the presence of BD.

Alves et al.[10] presented a kinetic model and the estimation of the corresponding parameters for BY hydrogenation on a commercial egg-shell catalyst, covering a temperature range of 27−62 °C. Experiments performed up to BY conversion of nearly 100% (i.e., when BY in the mixture reaches around 20 ppm) allowed identifying the (−1) and zeroth-order regimes that arise in the course of BY consumption. The results extended the preliminary kinetic identification reported by Alves et al.[11]

Alves et al.[12] carried out a complete kinetic characterization of the reactions in mixtures of BD and the three *n*-butene isomers on the same commercial catalyst used previously[10,11] at 44 °C. The effect of hydrogen partial pressures up to ∼10 atm was also quantified. Kinetic expressions were mainly derived from a mechanism of elementary steps proposed by Ardiaca et al.[13]

On the basis of the results of Alves et al.,[10,12] the specific goals of the present contribution are the following:

(a) Assembling a global mechanism and the corresponding set of kinetic expressions for systems presenting simultaneously both impurities, BY and BD, in mixtures of *n*-butenes (1BE, cBE, and tBE). New experiments at 44 °C are presented and analyzed for this purpose.

(b) Estimating the activation energies E_i of the kinetic coefficients of BD hydrogenation reactions and 1BE, cBE, and tBE hydrogenation and isomerization reactions from measurements performed in the range 25−65 °C, which is regarded as a temperature interval of practical significance in most industrial processes.

(c) Testing the overall performance of the kinetic model and estimated parameters on independent experiments. The results of two runs carried out until all unsaturated species are practically depleted at 25 and 65 °C are employed to this end.

The results of the present and previous contributions[10,12] allow fulfilling a general objective to have available a complete set of expressions and kinetic parameters for modeling the liquid-phase hydrogenation of relatively small amounts of BY and BD in *n*-butene-rich streams, in the temperature range of 25−65 °C. This achievement is expected to be useful for simulating the behavior of industrial reactors of selective hydrogenation, in particular for the preparation of high-purity 1-butene. Also discussed are the body of results and the strategy adopted for parameter fitting that can also be useful for commercial catalysts different from the one used for the present kinetic study.

2. EXPERIMENTAL SECTION

The experiments were carried out on a commercial Pd-based/Al_2O_3 egg-shell catalyst. Results from the catalyst characterization were reported by Bressa et al.[14]

Batch experiments with respect to the unsaturated hydrocarbons were performed using a laboratory reaction system with the main components sketched in Figure 1. The 100-mL

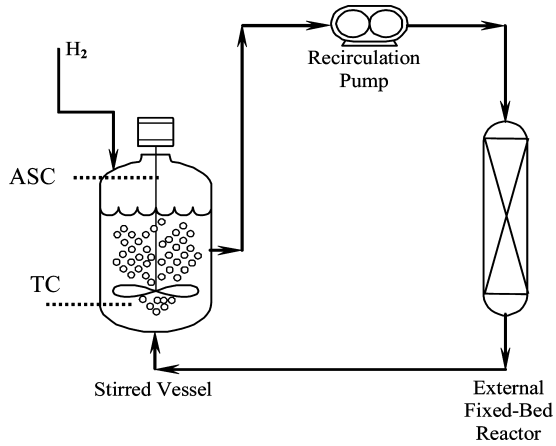

Figure 1. Recirculation system with an external fixed-bed reactor. ASC: agitation speed control, TC: temperature control.

stirred vessel (Autoclave Engineers EZE-Seal) was employed for different purposes such as loading the initial hydrocarbon mixture, feeding H_2 continuously, and maintaining the liquid saturated with H_2 during the runs. A gear micropump magnetically driven (Micropump 200) was used to recirculate at high rate (700 mL/min) the reaction mixture from the stirred vessel to the external fixed-bed reactor and back to the vessel. The external fixed-bed reactor consists of a 1/4-in.-o.d. stainless steel tube, which is filled with the desired amount of the catalyst sample. The catalyst pellets were loaded without milling, i.e. maintaining the original size. The high recirculation rate allowed minimizing external limitations to mass transfer toward the catalyst sample and keeping negligible per pass conversion.

Apart from the desired unsaturated hydrocarbons, *n*-hexane was used as an inert solvent to facilitate the manipulation of the samples analyzed chromatographically. Also, a certain amount of propane was employed for independent control of the hydrogen partial pressure and total pressure. The advantages of the outlined experimental set up were discussed by Ardiaca et al.[13]

A number of experimental details have been described or referenced recently,[10,12] such as sources of gases and hydrocarbons, purification procedure to avoid the introduction of moisture in the reacting mixture (moisture severely impairs the catalyst activity[15]), catalyst reduction and sampling procedures, chromatographic analysis, tests to ensure H_2 saturation in the reacting mixture, and absence of external and internal thermal effects.

dx.doi.org/10.1021/ie3029027 | Ind. Eng. Chem. Res. 2013, 52, 5849−5861

Table 1. Conditions of Experimental Runs

run	T [°C]	p_{H2} [atm]	$x_{BD,o}$ [%]	$x_{1BE,o}$ [%]	$x_{cBE,o}$ [%]	$x_{BY,o}$ [%]	M_c [g]	highlighted feature
1	44	1.47	5.69	0	0	1.99	0.90	catalyst selectivity for BD and BY hydrogenation
2	44	2.47	1.87	0	0	1.87	0.51	catalyst selectivity for BD and BY hydrogenation
3	27	3.71	9.62	0	0	0	0.38	temperature effect on BD reactions
	44	3.27						
	65	2.63						
4	25	3.42	0	9.59	0	0	0.50	temperature effects
	44	2.91						
5	44	2.95	0	0	8.40	0	0.50	temperature effects
	65	2.14						
6	64	2.64	1.80	10	0	0	0.50	testing the kinetic model
7	26	2.88	2.00	0	0	0	0.50	testing the kinetic model

3. GENERAL BEHAVIOR OF THE CATALYTIC SYSTEM

It was reported by Alves et al.[12] that in mixtures including BD (actually in all runs carried out in that contribution) a slow deactivation of the catalyst sample was observed when used for successive experiments. Also, some variations in catalytic activity were observed in runs performed with different catalyst samples. The problem was ascribed to the presence of 4-tert-butylcatechol (TBC)[16] in the cylinder that supplied BD. TBC is employed as a stabilizing agent for storing BD, as it inhibits BD polymerization. Clearly, as BD is loaded into the reaction system, TBC was also introduced. Its deactivation effect on Pd-based catalysts was reported e.g. by Nijhuis et al.[17] in a study of styrene hydrogenation.

Very fortunately, Alves et al.[12] could check that, irrespective of catalytic activity, different catalyst samples used with the same mixture composition showed essentially the same ratios between the different reaction rates. In other words, selectivity was maintained unaltered for any practical purpose. The analysis of the body of experimental results described in Alves et al.[12] could be performed without inconvenience by introducing a specific activity factor for each sample. The values of kinetic parameters reported by the authors were referred to the averaged activity factor among the different catalyst samples.

On the other hand, Alves et al.[10] found no deactivation and uniform catalytic activity from different samples in their kinetic study about BY hydrogenation. This finding can be easily explained by recalling that BY is not stored with TBC. In this contribution we will present experiments including simultaneously both BY and BD. The results from these experiments revealed that deactivation was not observed, that BY reacts at nearly the same rate as in the experiments without BD, and that the reactions that BD and the *n*-olefins (after BY depletion, see section 3) had undergone were faster than in the experiments without BY.

At present we have not investigated the reasons for this behavior, although it strongly suggests that the effect of TBC introduced with BD loading is neutralized by the presence of BY. If any homogeneous or catalytic reaction between BY and TBC is envisaged, only a negligible fraction of BY will suffice, due to the very small amount of TBC added with BD.

The quoted experiments including BY and BD allowed, as explained in more detail in section 5, identification of a level of catalytic activity unaffected by the presence of TBC, i.e. as it would be found for a catalyst in an industrial bed processing a stream without the presence of TBC.

Operating conditions of new experimental results to accomplish the goals of this contribution are listed in Table 1.

The behavior of mixtures containing BY, BD, and the three *n*-butene isomers reacting in the presence of H_2 on Pd catalysts can be described by the occurrence of the 10 reactions defined in Figure 2 (see e.g. Alves et al.[10,12]).

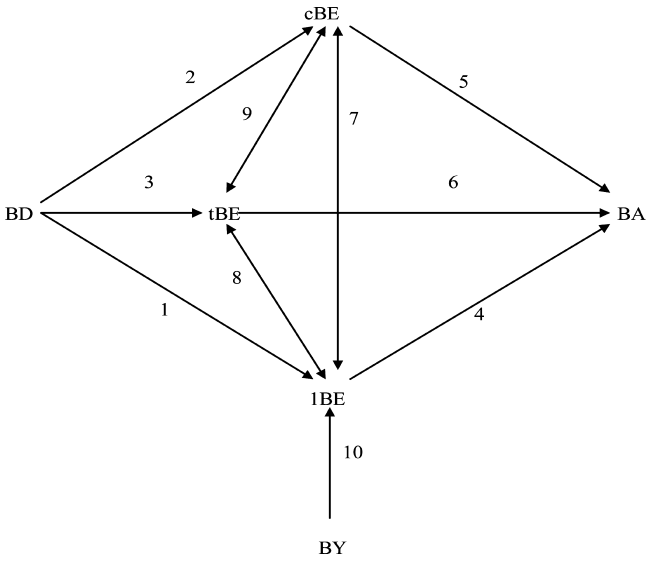

Figure 2. Scheme of global reactions.

The main features of the kinetic behavior shown by the hydrogenation of BD and BY over the commercial catalyst studied in this and in previous contributions[10−12,18] will be first summarized here. If any unsaturated species (BD, BY, 1BE, cBE, tBE) is present at concentrations above the detection threshold of our chromatographic analysis (about 50−100 ppm), it saturates by adsorption the active centers of the catalyst. However, the impurities BY and BD show much stronger adsorption strengths than any of the *n*-butenes (1BE, cBE, tBE). As a consequence, the concentration of BY and BD should drop below the mentioned threshold in order that *n*-butenes can compete for adsorption sites. As adsorption precedes hydrogenation (and isomerization among *n*-butenes), such features lead to the very high intrinsic selectivity shown by the catalyst for the hydrogenation of BY and BD.

On the other hand, the catalyst in the tested temperature range (25−65 °C) and hydrogen partial pressure level (above 1 atm) is fast enough to deplete any unsaturated species before this can reach the end of the active shell, provided that a surplus of dissolved hydrogen is present. This means that reactions proceed under strong diffusion limitations inside the active

dx.doi.org/10.1021/ie3029027 | Ind. Eng. Chem. Res. 2013, 52, 5849−5861

shell.[13] This feature brings a very important consequence for the observable selectivity. To explain this remark, it is first recalled that under the present experimental conditions mass transport inside the pores can be described by means of Fick's law (see e.g. Alves et al.[10]) and consequently the mass conservation equations allow reaching the conclusion that the limiting reactant will be defined as that showing the lower value of the product $D_j x_j$ (effective diffusivity times molar fraction at the catalyst surface). Then, if the product $x_{H2}D_{H2}$ evaluated at the catalyst surface is higher than $(x_{BY}D_{BY} + x_{BD}D_{BD})$, there will be an inner fraction of the catalytic shell free from BY and BD, and therefore the *n*-butenes will be able to adsorb and react with the H_2 surplus. In other words, hydrogenation and isomerization of the *n*-butenes will be observed even if in the liquid solution the concentration of BY and BD are high enough to avoid the adsorption and reactions of the *n*-butenes if they were in contact with the active centers.

Figure 3a, corresponding to run 1 listed in Table 1, is useful to illustrate the above-mentioned effects. Until the reaction time indicated by the dashed vertical line (t^*), the constant amount of H_2 dissolved is such that $x_{H2}D_{H2} < (x_{BY}D_{BY} + x_{BD}D_{BD})$. Hence, H_2 is the limiting reactant, and the impurities (either BY or BD) can cover essentially all active sites within the catalytic shell. The *n*-butenes that appear from the hydrogenations of BY and BD (reactions 1−3 and 10 in Figure 2) behave strictly as "reaction products". Among them, 1BE is favored as it is the main product from BD hydrogenation, and it is the only product from BY hydrogenation.

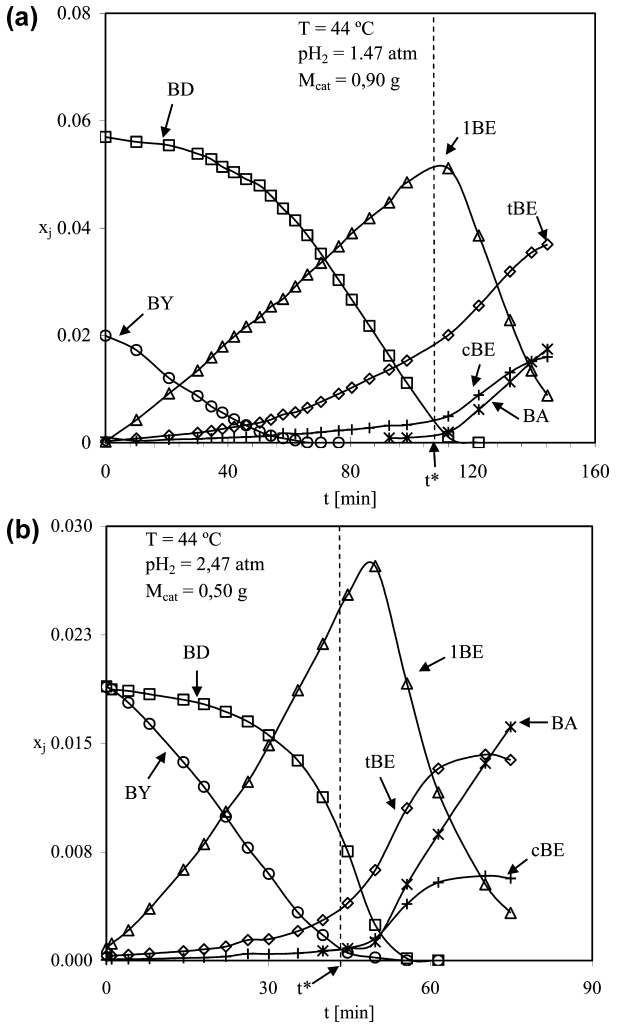

Figure 3. (a) Hydrocarbon mole fractions vs reaction time (run 1 in Table 1). (b) Hydrocarbon mole fractions vs reaction time (run 2 in Table 1).

It can be observed that in this initial period of time BD and BY react simultaneously, showing that they can compete, up to a certain degree, for the same active sites. BY, while being alone and in excess with respect to hydrogen, reacts following a (−1) reaction order up to very small concentrations.[10,11] Instead, BD at similar conditions reacts following a zeroth-order reaction. The concavity of the x_{BD} trajectory suggests that BD adsorption, even when being more concentrated than BY, is significantly impaired by the presence of BY. We can conclude as a trend that BY can be adsorbed more strongly than BD, but still BD is able to occupy a certain fraction of active sites.

After the initial period, i.e. when $x_{H2}D_{H2} > (x_{BY}D_{BY} + x_{BD}D_{BD})$, the *n*-butenes can adsorb and react. As 1BE shows higher adsorption strength than the other isomers (relative values of adsorption constants obtained by Alves et al.[12] are $K_{cBE}/K_{1BE} = 0.64$, $K_{tBE}/K_{1BE} = 0.27$) and reaches the highest concentration after the initial period, it behaves as the most reactive isomer and is monotonically consumed during the second period.

At somewhat longer times than the sampling times in Figure 3a (say, >160 min), the hydrogenation rates of cBE and tBE exceed their production from 1BE, and they start to be hydrogenated until complete disappearance, when BA becomes the only C4 hydrocarbon remaining in the mixture. To complete this introductory description, it is pointed out that any of the *n*-butenes will react following a zeroth-order reaction if it is in excess with respect to hydrogen and at very small concentrations of the remaining two isomers.[12]

The same conclusions can be obtained from the results in Figure 3b, corresponding to run 2, listed in Table 1.

4. KINETIC MODEL

A kinetic model to quantify the trends discussed in General Behavior of the Catalytic System, section 3, can be formulated by simultaneous consideration of the mechanisms proposed by Alves et al.[12] to model hydrogenation of BD and hydrogenation/isomerization of *n*-butenes and the mechanism used by Alves et al.[10] for the hydrogenation of BY. The results discussed in section 3 strongly suggest that all hydrocarbon species react after initial adsorption on the same active sites of the catalysts. Therefore, the basis for the present proposal stems from considering that all elementary steps in the mechanisms of Alves et al.[10,12] can take place simultaneously in a system composed of BY, BD, and *n*-butenes.

In the work of Alves et al.[12] two different alternatives were proposed for the course of BD reactions. The difference arises from the assumption regarding the BD adsorption step, either on a single[14,19] or on two neighboring active sites. The goodness of fit for both approaches was statistically the same, and therefore the set of kinetic expressions derived from them could not be discriminated. Here we assume a single active site for BD adsorption because slightly simpler expressions arise for reaction rate expressions.

The 18 elementary steps thus resulting are listed in Figure 4. They will be described briefly in the following paragraphs, for the sake of completeness, but more details and considerations can be found in the original references.[10,12]

dx.doi.org/10.1021/ie3029027 | Ind. Eng. Chem. Res. 2013, 52, 5849−5861

a) $H_2 + 2\odot \leftrightarrow 2H\odot$

b) $BD + \times \leftrightarrow \times BD$

c) $BY + \times \leftrightarrow \times BY$

d) $\times BY + BY \leftrightarrow \times(BY)_2$

e) $1BE + \times \leftrightarrow \times 1BE$

f) $cBE + \times \leftrightarrow \times cBE$

g) $tBE + \times \leftrightarrow \times tBE$

h) $\times BD + H\odot \leftrightarrow \times C_4H_7 + \odot$

i) $\times BY + H\odot \leftrightarrow \times(C_4H_7)^{BY} + \odot$

j) $\times C_4H_7 + H\odot \rightarrow \times 1BE + \odot + \times$

k) $\times C_4H_7 + H\odot \rightarrow \times cBE + \odot + \times$

l) $\times C_4H_7 + H\odot \rightarrow \times tBE + \odot + \times$

m) $\times(C_4H_7)^{BY} + H\odot \rightarrow \times 1BE + \odot$

n) $\times 1BE + H\odot \leftrightarrow \times C_4H_9{}^1 + \odot$

o) $\times 1BE + H\odot \leftrightarrow \times C_4H_9{}^2 + \odot$

p) $\times cBE + H\odot \leftrightarrow \times C_4H_9{}^2 + \odot$

q) $\times tBE + H\odot \leftrightarrow \times C_4H_9{}^2 + \odot$

r) $\times C_4H_9{}^1 + H\odot \leftrightarrow BA + \times + \odot$

s) $\times C_4H_9{}^2 + H\odot \leftrightarrow BA + \times + \odot$

Figure 4. Elementary reaction steps of the proposed mechanism.

Steps a−g account for adsorption of all reactive species. A dissociative adsorption step[20,21] is assumed for H_2 (step a) in Figure 4 on sites identified by (⊙), which are different from the sites (X) involved in the adsorption of hydrocarbon species. This hypothesis assumes that, when hydrocarbon species are adsorbed, even at the extent of saturation, free interstitial sites remain accessible for the very small H_2 molecules, but not for additional molecules of the bulkier hydrocarbons. This noncompetitive adsorption hypothesis is widely accepted in literature, as was pointed out by Boitiaux et al.,[3] Bressa et al.,[14] and references therein.

The unsaturated hydrocarbon species adsorb on a single active center (X), with the exception of BY that, in addition, can adsorb to form a more stable complex consisting of two molecules of BY adsorbed on a single site, step d. This step allows accounting for the (−1) reaction order observed for the hydrogenation of BY,[3,4] provided that the adsorbed complex, $X(BY)_2$ is regarded as being nonreactive.

The remaining steps in Figure 4 involve surface reactions that in turn can be divided into two groups. On one hand, every adsorbed species [except $X(BY)_2$] undergoes a semihydrogenation reaction, steps h, i, n−q, rendering semihydrogenated surface intermediates. In the second group, these intermediates further react with an additional adatom ⊙H to form either adsorbed unsaturated species (steps j−m) or release BA into the liquid phase inside the pores (steps r, s). The adsorbed 1-butene species, X1BE, can follow two alternative routes for its first ⊙H uptake, producing either a radical in position 1, $XC_4H_9{}^1$ (step n), or in position 2, $XC_4H_9{}^2$ (step o).

To obtain the kinetic expressions from the mechanism in Figure 4, the following assumptions were made:

(1) Adsorption steps a−g in Figure 4 are fast enough to be regarded as being in quasi-equilibrium.

(2) The amount of sites "X" engaged with the semihydrogenated surface intermediates XC_4H_7, $X(C_4H_7)^{BY}$, $XC_4H_9{}^1$, and $XC_4H_9{}^2$ can be neglected in relation to the total amount of sites $[X]_T$.

The resulting expressions in terms of the 10 overall reactions displayed in Figure 2 are gathered in Figure 5, in which y_j stands for the local molar fraction of species j inside the pores of the active shell.

The expressions take the LHHW form, with all driving forces being linear in concentrations of hydrocarbon species. A linear factor y_{H2} arises in all hydrogenation reactions, and a factor $y_{H2}{}^{0.5}$ in all isomerization reactions. There is a single inhibition term related to the finite surface concentration of X sites

$$r_1 = \frac{k_1 K_{BD} y_{BD} y_{H2}}{DEN_{HC} DEN_{H2} DEN_{H2}^{\alpha}} \quad r_2 = \frac{k_2 K_{BD} y_{BD} y_{H2}}{DEN_{HC} DEN_{H2} DEN_{H2}^{\alpha}} \quad r_3 = \frac{k_3 K_{BD} y_{BD} y_{H2}}{DEN_{HC} DEN_{H2} DEN_{H2}^{\alpha}}$$

$$r_4 = \left(\frac{k_4^{I}}{DEN_{H2}^{\beta}} + \frac{k_4^{II}}{DEN_{H2}^{\gamma}}\right) \frac{k_1 K_{1BE} y_{1BE} y_{H2}}{DEN_{HC} DEN_{H2}} \quad r_7 = \frac{k_7 K_{1BE} \sqrt{y_{H2}}}{DEN_{HC} DEN_{H2} DEN_{H2}^{\gamma}} \left[y_{1BE} + \frac{y_{cBE}}{K_{1\text{-}c}^{eq}}\right]$$

$$r_5 = \frac{k_5 K_{cBE} y_{cBE} y_{H2}}{DEN_{HC} DEN_{H2} DEN_{H2}^{\gamma}} \quad r_8 = \frac{k_8 K_{1BE} \sqrt{y_{H2}}}{DEN_{HC} DEN_{H2} DEN_{H2}^{\gamma}} \left[y_{1BE} + \frac{y_{tBE}}{K_{1\text{-}t}^{eq}}\right]$$

$$r_6 = \frac{k_6 K_{tBE} y_{tBE} y_{H2}}{DEN_{HC} DEN_{H2} DEN_{H2}^{\gamma}} \quad r_9 = \frac{k_9 K_{cBE} \sqrt{y_{H2}}}{DEN_{HC} DEN_{H2} DEN_{H2}^{\gamma}} \left[y_{cBE} + \frac{y_{tBE}}{K_{c\text{-}t}^{eq}}\right]$$

$$r_{10} = \frac{k_{10} K_{BY} y_{BY} y_{H2}}{DEN_{HC} DEN_{H2} DEN_{H2}^{\varphi}}$$

Hydrocarbon inhibition terms

$$DEN_{HC} = 1 + K_{BY} K_{\eta} y_{BY}^2 + \sum_{j=1BE,\ cBE,\ tBE,\ BD,\ BY} K_j y_j$$

Hydrogen inhibition terms

$$DEN_{H2} = 1 + \sqrt{K_{H2} y_{H2}} \qquad DEN_{H2}^{\alpha} = 1 + \alpha \sqrt{y_{H2}}$$

$$DEN_{H2}^{\beta} = 1 + \beta \sqrt{y_{H2}} \qquad DEN_{H2}^{\gamma} = 1 + \gamma \sqrt{y_{H2}} \qquad DEN_{H2}^{\varphi} = 1 + \varphi \sqrt{y_{H2}}$$

Figure 5. Kinetic expressions derived from the reaction mechanism.

(DEN_{HC}), which depends on the concentrations of all unsaturated species, and there are five terms associated with y_{H2}: DEN_{H2} arises from the finite amount of sites ⊙, and DEN_{H2}^{α}, DEN_{H2}^{β}, DEN_{H2}^{γ}, and DEN_{H2}^{φ} arise from imposing a null net rate of formation of the semihydrogenated surface intermediates.

Parameters Estimated at 44 °C in Previous Contributions. In principle, fitting parameters from the set of expressions in Figure 5 are the kinetic coefficients k_i, adsorption constants K_j, and the parameters α, β, γ, φ of the H_2 inhibition terms. On the other hand, the equilibrium constants of isomerization reactions, $K_{1,c}^{eq}$, $K_{1,t}^{eq}$, and $K_{c,t}^{eq}$ are evaluated from thermodynamic properties at each operating temperature.

The kinetic parameters introduced in the expressions of Figure 5 are related to the kinetic parameters of the individual elementary step of the mechanism in Figure 4. From such relationships, it can be concluded[14] that three combinations arise among the coefficients in Figure 5. They can be written as

$$k_4^{II} = \frac{k_5 k_8}{k_9}; \quad k_6 = \frac{K_{cBE}}{K_{tBE}} \frac{k_5 k_8}{k_7 K_{c,t}^{eq}}$$

$$\gamma = \frac{k_5}{k_9(1 + k_7/k_8) + \frac{k_7}{K_{1-c}^{eq}} \frac{K_{1BE}}{K_{cBE}}} \qquad (1)$$

Therefore, coefficients k_4^{II}, k_6, and γ are not regarded as being independent in the fitting procedure (see e.g. Alves et al.[12]).

The estimation of the independent fitting parameters have been undertaken from a large collection of experimental data at 44 °C.[10,12] The specific temperature of 44 °C was chosen as being midway within the temperature range of practical interest.

Some relevant features arising from the study of Alves et al.[10,12] are worth noting here.

Parameters K_{H2}, α, β, and φ could not be statistically distinguished from zero. Hence, in using the expressions in Figure 5,

$$DEN_{H2} = DEN_{H2}^{\alpha} = DEN_{H2}^{\beta} = DEN_{H2}^{\varphi} = 1 \qquad (2a)$$

dx.doi.org/10.1021/ie3029027 | Ind. Eng. Chem. Res. 2013, 52, 5849−5861

should be taken. Failure in fitting such parameters was most probably due to the level of hydrogen partial pressure, which remained less than around 10 atm. From a practical point of view, it should be born in mind, as discussed in Alves et al.,[10,12] that higher hydrogen partial pressures will severely impair the selectively of the process, allowing high rates of hydrogenation and isomerization of the *n*-olefins before the extinction of BY and BD.

Although some of the experiments were conducted near the limit of practical detection of the unsaturated species, the hydrocarbon inhibition term DEN_{HC} turns out to be always much larger than one, which means that, in spite of the low concentration of the unsaturated species, the catalyst surface was fully covered by adsorbed compounds. Therefore, in practical terms we have that

$$DEN_{HC} = K_{BY}K_{\eta}y_{BY}^2 + \sum_{j=1BE,cBE,tBE,BD,BY} K_j y_j \quad (2b)$$

An inspection of the kinetic expressions in Figure 5 with DEN_{HC} given in eq 2b reveals that the ratios between the adsorption constants K_j can be estimated, but not their absolute values. On the other hand, it is concluded that the adsorption constant K_η is the only one that can be estimated individually.

The values at 44 °C, k_{10} and K_η from Alves et al.[10] and k_i (i = 1−9), K_{BD}/K_{1BE}, K_{cBE}/K_{1BE}, and K_{tBE}/K_{1BE} from Alves et al.[12] are gathered in Table 2. It must be mentioned that k_i values (i = 1−9) reported in Table 2 have been rescaled, according to the procedure discussed in section 5. Also, for the sake of completeness, Table 2 includes the relation K_{BY}/K_{BD} obtained from the experiments and regression analysis introduced in this study (sections 5 and 6).

Table 2. Optimal Values and Confidence Intervals of Kinetic Parameters at 44 °C, as Estimated by Alves et al.,[10,12] except the Value (K_{BY}/K_{BD}) (Estimated in the Present Contribution)[a]

Kinetic Coefficients, k_i = [mol/(m^3_{shell} s)]	
$k_1 = 4.29\ (1 \pm 0.036) \times 10^5$	$k_5 = 2.72\ (1 \pm 0.20) \times 10^5$
$k_2 = 3.49 \times 10^4$[a]	$k_7 = 1.75\ (1 \pm 0.20) \times 10^4$
$k_3 = 1.95\ (1 \pm 0.06) \times 10^5$	$k_8 = 1.72\ (1 \pm 0.16) \times 10^4$
$k_4^I = 5.79\ (1 \pm 0.14) \times 10^5$	$k_9 = 2.25\ (1 \pm 0.18) \times 10^4$
$k_{10} = 2.44\ (1 \pm 0.0041) \times 10^6$	
Dependent Parameters (see eq 1 in the text)	
$k_4^{II} = 2.08 \times 10^5$, $k_6 = 2.31 \times 10^5$, $\gamma = 5.7$	
Adsorption Constants	
$K_{BD}/K_{1BE} = 1.74\ (1 \pm 0.63) \times 10^3$	$K_{BY}/K_{BD} = 1.18\ (1 \pm 0.13)$
$K_{cBE}/K_{1BE} = 0.64\ (1 \pm 0.47)$	$K_\eta = 2.27\ (1 \pm 0.009) \times 10^2$
$K_{tBE}/K_{1BE} = 0.27\ (1 \pm 0.59)$	

[a]The confidence interval of k_2 could not be evaluated, as explained by Alves et. al.[12]

5. EXPERIMENTAL RESULTS INTRODUCED IN THIS CONTRIBUTION

The experiments reported in this contribution pursued three objectives. On one hand, estimating the ratio between the adsorption constants of BY and BD, K_{BY}/K_{BD}, at 44 °C and rescaling the kinetic coefficient k_i (i = 1−9) from Alves et al.[12] Second, estimating the activation energy of the kinetic coefficients k_i (i = 1−9). The final goal is testing the kinetic model against experiments that were not involved in parameter estimation.

To accomplish the first objective, runs 1 and 2 (Table 1) were performed. Both runs differ in the ratio between BY and BD initial concentrations and in the level of H_2 partial pressure. The results from run 1 are presented in Figure 3a and those from run 2 in Figure 3b. Continuous lines were drawn in Figures 3a and 3b with the purpose of improving clarity. Considering the aim of these two runs, the relevant data are those when BD and BY are reacting simultaneously. As BY extinguishes first, the relevant data are those up to about 70 min for run 1 and up to around 50 min for run 2. In practice, during these periods of time, a combination of BY and BD saturates the active sites. Thus, only reactions 1, 2, 3, and 10 (Figure 2) take place at significant rates that, according to Figure 5 and the approximation given by eqs 2a and 2b, can be written locally inside the active shell as

$$r_i = \frac{k_i y_{BD} y_{H2}}{y_{BD} + (K_{BY}/K_{BD})y_{BY} + (K_{BY}/K_{BD})K_\eta y_{BY}^2} \quad i = 1, 2, 3 \quad (3)$$

$$r_{10} = \frac{k_{10}(K_{BY}/K_{BD})y_{BY}y_{H2}}{y_{BD} + (K_{BY}/K_{BD})y_{BY} + (K_{BY}/K_{BD})K_\eta y_{BY}^2} \quad (4)$$

Defining $r_{BD}=r_1 + r_2 + r_3$ (the overall BD consumption rate), we obtain from eqs 3 and 4

$$r_{BY}/r_{BD} = (k_{10}/k_{BD})(K_{BY}/K_{BD})(y_{BY}/y_{BD}) \quad (5)$$

where $k_{BD}=k_1 + k_2 + k_3$. As k_{10} and k_{BD} could be well estimated from previous experiments and the data from runs 1 and 2 allow a proper quantification of r_{BY}/r_{BD}, eq 5 reveals that these experiments can provide a suitable estimation of the ratio (K_{BY}/K_{BD}). It is noted, however, that eq 5 is used at this point to highlight the suitability of the experiments for identification of the ratio(K_{BY}/K_{BD}), but the actual regression analysis was carried out using the entire kinetic model (Figure 5).

As commented on in section 3, experiments with the presence of BY showed a high and stable catalytic activity, as compared with experiments in which BD was the only impurity added to the initial mixture. The analysis of the results from runs 1 and 2 allowed rescaling the values of kinetic coefficients k_i (i = 1−9) reported by Alves et al.[12] to the (high) level of catalytic activity when BY is included in the reacting mixture. This was achieved by using a single scaling factor for all k_i (i = 1−9).

For the objective of estimating activation energies, runs 3, 4, and 5 of Table 1 were employed.

Run 3, employing a high initial concentration of BD as the only initial reactant, was intended for evaluation of the activation energy of k_1, k_2, and k_3 (Figure 5). In this experiment the temperature was raised in three steps (27, 44, and 65 °C), as shown in Figure 6a. This procedure allowed evaluating the effect of temperature on the same catalyst sample, avoiding the risk of changes in catalytic activity if different samples would have been employed (see section 3).

As can be appreciated in Figure 6a, H_2 partial pressure decreases after each temperature step. This is a consequence of operating at constant total pressure and the simultaneous rise of the hydrocarbon partial pressures following the temperature steps. Although the solubility of H_2 increases slightly with temperature, the net effect was a drop of H_2 molar fraction in

dx.doi.org/10.1021/ie3029027 | Ind. Eng. Chem. Res. 2013, 52, 5849−5861

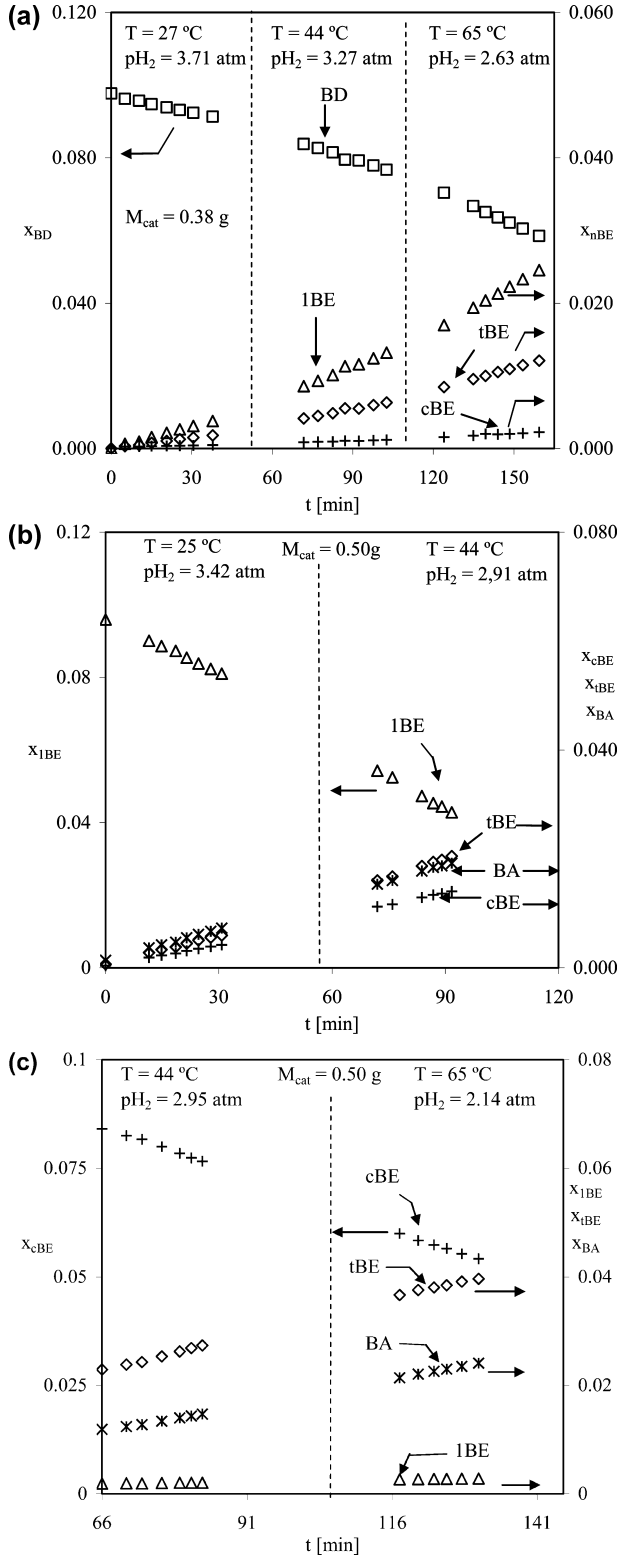

Figure 6. (a) BD, 1BE, cBE, and tBE mole fractions vs reaction times for three levels of temperatures (high BD initial concentration, run 3 in Table 1). (b) 1BE, cBE, tBE, and BA mole fractions vs reaction times for two levels of temperatures (high 1BE initial concentration, run 4 in Table 1). (c) 1BE, cBE, tBE, and BA mole fractions vs reaction times for two levels of temperatures (high cBE initial concentration, run 5 in Table 1).

the liquid mixture at each temperature step (10^3 x_{H2} = 3.15, 2.91, 2.55 at 27, 44, 65 °C, respectively).

At the end of the run, BD concentration is still higher than the dissolved H_2 concentration (Figure 6a). Therefore, during the whole run only reactions 1, 2, and 3 in Figure 2 take place under zero order with respect to BD. Thus, according to the expressions in Figure 5 and the approximations given by eqs 2a and 2b we can write locally inside the active shell

$$r_i = k_i y_{H2}; \quad i = 1, 2, 3 \tag{6}$$

With the main purpose of identifying the activation energy of kinetic coefficients corresponding to 1BE hydrogenation and isomerization (reactions 4, 7, and 8 in Figure 2), run 4 was performed with highly concentrated 1BE as the only initial reactant. As for run 3, temperature was raised in steps. In this case, only two temperature levels were employed, 25 and 44 °C (see Figure 6b). Due to the high 1BE concentration along the run, 1BE is in excess with respect to H_2, and it can be assumed that 1BE saturates the active catalyst sites, a case in which reactions 4, 7, and 8 will proceed locally inside the active catalytic shell according to the expressions in Figure 5 and the approximations given by eqs 2a and 2b:

$$r_4 \approx \left(k_4^{I} + \frac{k_4^{II}}{DEN_{H2}^{\gamma}}\right) y_{H2}$$

$$r_7 \approx \frac{k_7\sqrt{y_{H2}}}{DEN_{H2}^{\gamma}}\left[1 - \frac{y_{cBE}}{y_{1BE}K_{1-c}^{eq}}\right]$$

$$r_8 \approx \frac{k_8\sqrt{y_{H2}}}{DEN_{H2}^{\gamma}}\left[1 - \frac{y_{tBE}}{y_{1BE}K_{1-t}^{eq}}\right] \tag{7}$$

In the regression analysis, reactions 5, 6, and 9 (hydrogenation of cBE and tBE and isomerization between them) were also considered. However, the kinetic behavior of the run was approximately governed by expressions 7, revealing that the results from this experiment are sensitive to the activation energy of k_4^{I} (k_4^{II} is a dependent parameter, see eq 1), k_7, and k_8.

Run 5, in a fashion similar to that of runs 3 and 4, was carried out with a high initial concentration of cBE. The run was started at 25 °C, but the corresponding liquid samples for chromatographic analysis were accidentally lost. In consequence, only the results at 44 and 65 °C shown in Figure 6c remained available. In this case, the run was kinetically governed by expressions (cf. eq 7):

$$r_5 \approx k_5 y_{H2} \qquad r_7 \approx \frac{k_7\sqrt{y_{H2}}}{DEN_{H2}^{\gamma}}\left[\frac{y_{1BE}}{y_{cBE}} - \frac{1}{K_{1-c}^{eq}}\right]$$

$$r_9 \approx \frac{k_9\sqrt{y_{H2}}}{DEN_{H2}^{\gamma}}\left[1 - \frac{y_{tBE}}{y_{cBE}K_{c-t}^{eq}}\right] \tag{8}$$

The effects of coefficients k_5, k_7, and k_9 were expected to become evident in this case. However, in practice, isomerization of cBE to 1BE does not take place significantly, as this reaction is not favored kinetically nor thermodynamically with respect to isomerization of cBE to tBE, as can be appreciated from the low amount of 1BE formed. (Figure 6c). Then, the activation energy of k_7 was chiefly estimated from the results of run 4.

The activation energy corresponding to all reactions 1−9 in Figure 2 can be suitably estimated from the results of runs 3, 4, and 5, if we recall that k_6 is evaluated as a dependent parameter (eq 1).

dx.doi.org/10.1021/ie3029027 | Ind. Eng. Chem. Res. 2013, 52, 5849−5861

Runs 6 and 7 in Table 1, at 64 and 26 °C, respectively, were performed to validate the set of estimated parameters with independent experiments. These were conducted almost up to total consumption of unsaturated species to highlight the occurrence of reactions 1−9 (see Figure 2), i.e. all reactions except for BY hydrogenation (reaction 10).

6. REGRESSION OF EXPERIMENTAL DATA AND RESULTS FOR THE FITTING PARAMETERS

For regression of the experimental data, the set of molar fractions at the different sampling times were compared with the values arisen from modeling the experiments. The regression analysis was performed with GREGPAK,[22] employing the solver GREG in the nonlinear multiresponse Bayesian mode with the determinant of the residual matrix as the objective function for minimization (determinant criterion).

A number of aspects to generate the model responses were recently described by Alves et al.[10,12] These include vapor equilibrium calculations to obtain the composition and amount of the bulk liquid reacting mixture, in particular the H_2 solubility and the evaluation of transport parameters (effective diffusivities inside the active shell and mass transfer coefficients to account for the moderate external effects). Therefore, we will only outline here the essential features of the model employed to generate the predicted response at each reaction time.

Assuming uniform composition in the whole loop depicted in Figure 1, the global mole fractions x_j of the hydrocarbon species were evaluated from solving the mass conservation equations in the liquid bulk:

$$N_T \frac{dx_j}{dt} = -V_{shell} R_j \tag{9}$$

where N_T is the total number of moles remaining in the loop after the extraction of each sample for chromatographic analysis, V_{shell} is the total volume of active shells of the catalyst sample in the fixed bed (Figure 1), and R_j the effective rate of consumption of species j for a trial set of values of the kinetic parameters (Figure 5).

The values R_j were evaluated from solving the conservation equations inside the active shell:

$$D_j C_T \, d^2 y_j/dz^2 = L_{ac}{}^2 r_j \tag{10}$$

where D_j is the effective diffusivity of j, C_T the total molar concentration, L_{ac} the length of active shell, z the dimensionless coordinate inside the shell, and r_j is the local consumption rate of species j, expressed from the local reaction rates r_i (Figure 2 and Figure 5). For example, for 1BE: $r_{1BE} = r_4 + r_7 + r_8 - r_1 - r_{10}$.

Boundary conditions for eq 10 are:

$$D_j \, dy_j/dz = L_{ac}\kappa_j(x_j - y_j); \quad z = 1 \tag{11a}$$

$$dy_j/dz = 0; \quad z = 0 \tag{11b}$$

In eq 11a, κ_j is the external mass transfer coefficient. The set of eqs 10, 11a, and 11b were solved with the code described by Bressa et al.[23] Finally,

$$R_j = \int_0^1 r_j \, dz \tag{12}$$

As stated in section 5, runs 1 and 2 were employed for estimating the ratio K_{BY}/K_{BD} =1.18 (1 ± 0.13) at 44 °C (also reported in Table 2). Only two fitting parameters were used in the regression procedure, K_{BY}/K_{BD} and the catalytic activity factor to obtain the rescaled kinetic coefficients k_i (i = 1−9) given in Table 2.

The temperature dependence of kinetic coefficients was expressed as

$$k(T) = k(T_{ref}) \exp\left[-\frac{E}{R}\left(\frac{1}{T} - \frac{1}{T_{ref}}\right)\right] \tag{13}$$

where E represents the activation energy and T_{ref} = (44 + 273) K is the reference temperature. Expressing the temperature dependence of kinetic coefficients as in eq 13 lessens the strong correlation between the pre-exponential factor and the activation energy in Arrhenius-type expressions.[24]

In the regression analysis, $k_i(T_{ref})$ were fixed at the values in Table 2, and a fitting activity factor was introduced for each run (3, 4, and 5 in Table 1).

The reduced expressions, eq 6, were used to estimate E_i (i = 1−3) from the data of run 3. For estimating activation energies of hydrogenation and isomerization reactions of the *n*-butenes (from runs 4, 5) the full kinetic expressions in Figure 5 for reactions 4−9 (and the approximations given by eqs 2a and 2b) were used, for which the ratios of adsorption constants K_{cB}/K_{1BE} and K_{tBE}/K_{1BE} were taken at 44 °C (Table 2).

In summary, the fitting parameters in the analysis of runs 3, 4, and 5 in Table 1 were the activation energies and a catalytic activity factor for each run. The results for E_i and their confidence limits are listed in Table 3, which includes also the values of E_{10} and ΔH_η (corresponding to K_η), as reported by Alves et al.[10]

Table 3. Optimal Values and Confidence Intervals of Activation Energies E_i [J/mol], and Enthalpy of Adsorption ΔH_η [J/mol] of K_η, E_{10} and ΔH_η from Alves et al.,[10] and the Remaining Parameters Are Estimated in the Present Contribution

E_1 = 3.98 (1 ± 0.04) × 10^4	E_7 = 4.65 (1 ± 0.05) × 10^4
E_2 = 4.73 (1 ± 0.09) × 10^4	E_8 = 4.52 (1 ± 0.06) × 10^4
E_3 = 3.96 (1 ± 0.04) × 10^4	E_9 = 1.71 (1 ± 0.35) × 10^4
E_4^1 = 2.09 (1 ± 0.12) × 10^4	E_{10} = 3.18 (1 ± 0.08) × 10^4
E_5 = 3.93 (1 ± 0.12) × 10^4	ΔH_η = −3.39 (1 ± 0.10) × 10^4

7. DISCUSSION ABOUT THE SIGNIFICANCE OF THE AVAILABLE SET OF KINETIC PARAMETERS

First, we will discuss briefly the "goodness of fit" achieved from the regression of the experimental data presented in this work. After that, a general discussion will be undertaken about the whole set of parameters available to modeling the behavior of the selective hydrogenation system.

Figures 7 and 8 compare the experimental data in runs 1 and 2 with model predictions after parameter fitting (K_{BY}/K_{BD} and the catalytic activity factor). The discontinuity in the model prediction for an intermediate time interval in Figure 8 is due to a failure in the solver for the internal conservation balances (eqs 10, 11a, and 11b). It can be appreciated that the evolution of BY and BD mole fractions are very well represented by the model in both experiments (runs 1, 2 in Table 1), as reflected by the low uncertainty in the estimation of K_{BY}/K_{BD}: ± 13% (see Table 2). Also, the distribution of the *n*-butenes and the generation of BA after depletion of BY and BD can be visually

dx.doi.org/10.1021/ie3029027 | Ind. Eng. Chem. Res. 2013, 52, 5849−5861

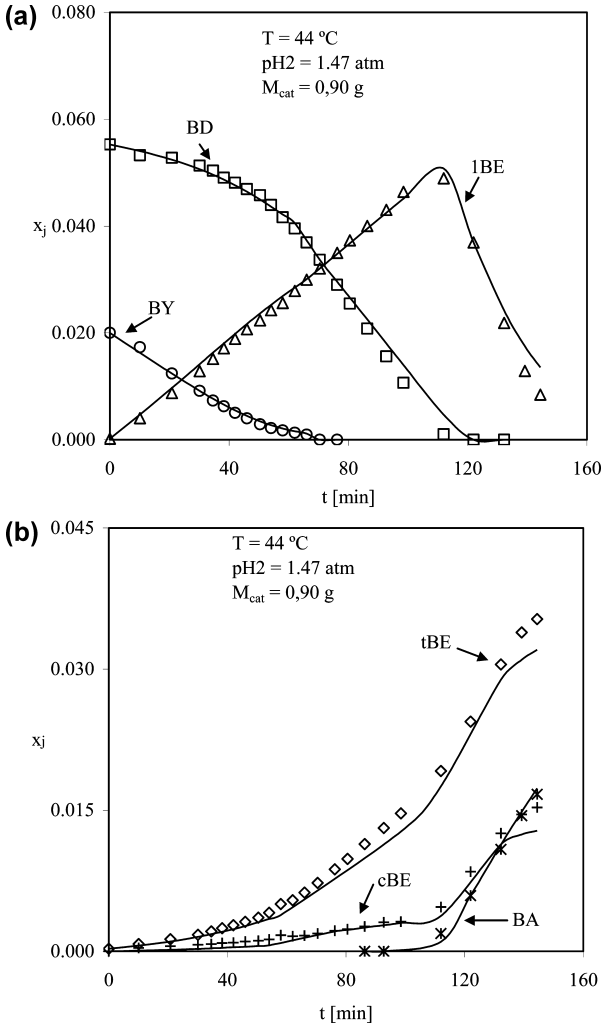

Figure 7. (a) Comparison of experimental (symbols) and model results (continuous lines) for run 1 in Table 1. BY, BD, and 1BE mole fractions vs reaction time. (b) Comparison of experimental (symbols) and model results (continuous lines) for run 1 in Table 1. BA, cBE, and tBE mole fractions vs reaction time.

judged as being satisfactory, revealing the adequacy of the set of parameters previously determined[12] after fitting a single value of catalytic activity factor for all kinetic coefficients. The overall relative difference between concentrations measured and predicted from runs 1 and 2 is ε = 5.1%.

A good matching between experimental data and model predictions for run 3, intended for estimating the activation energies E_i (i = 1−3) can be appreciated in Figure 9. Similar behavior is revealed from runs 4 and 5 for estimating the activation energy of *n*-butenes reactions. The overall relative difference of the five responses (mole fractions of BD, 1BE, cBE, tBE, BA) for the set of runs 3, 4, and 5 was ε = 2.71%, and no systematic deviation was observed.

The set of estimated activation energies displayed in Table 3 shows acceptable confidence limits, except that for reaction 9 (isomerization between cBE and tBE), a feature that is probably related to the low modal value of E_9. It should be remarked, however, that few experimental temperature levels were employed. In particular, the values of activation energies for the *n*-butenes' reactions were obtained from only two temperatures levels (runs 3 and 4); hence, the confidence intervals are not related to the adequacy of Arrhenius law but

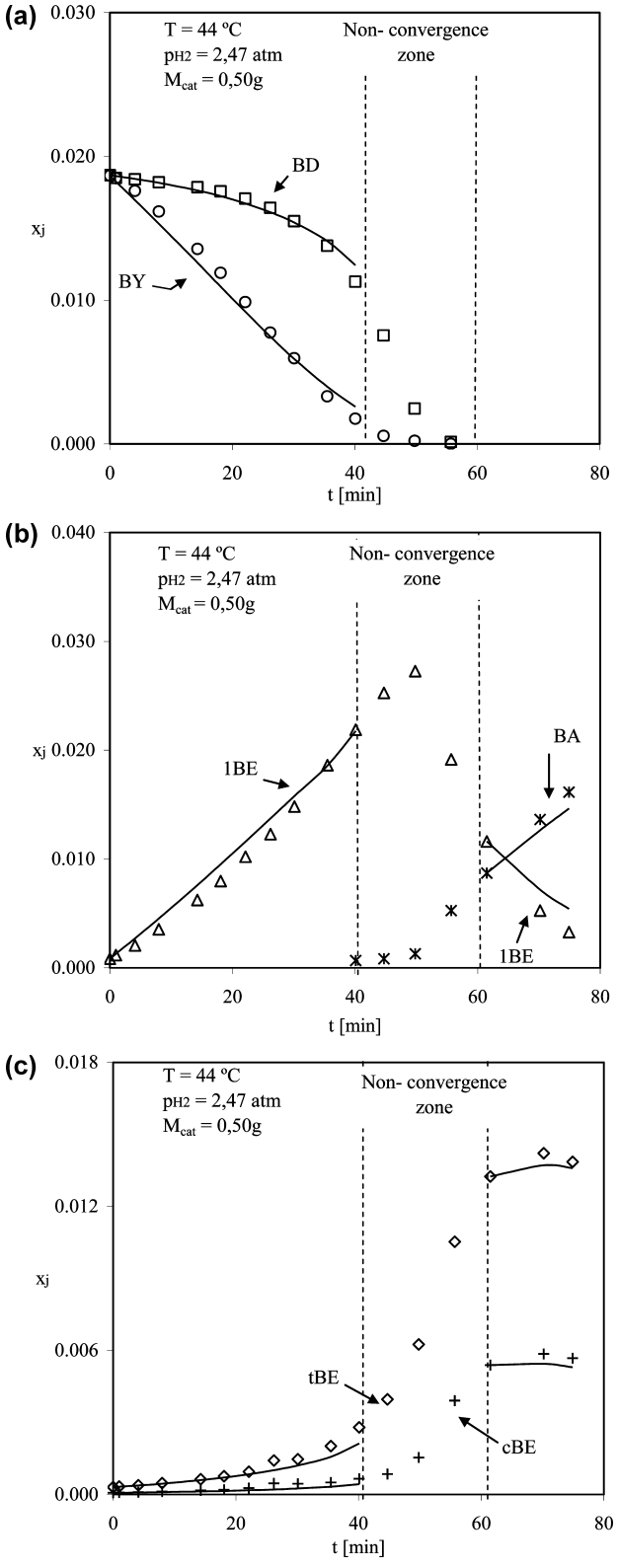

Figure 8. (a) Comparison of experimental (symbols) and model results (continuous lines) for run 2 in Table 1. BY and BD mole fractions vs reaction time. (b) Comparison of experimental (symbols) and model results (continuous lines) for run 2 in Table 1. 1BE and BA mole fractions vs reaction time. (c) Comparison of experimental (symbols) and model results (continuous lines) for run 2 in Table 1. tBE and cBE mole fractions vs reaction time.

dx.doi.org/10.1021/ie3029027 | Ind. Eng. Chem. Res. 2013, 52, 5849−5861

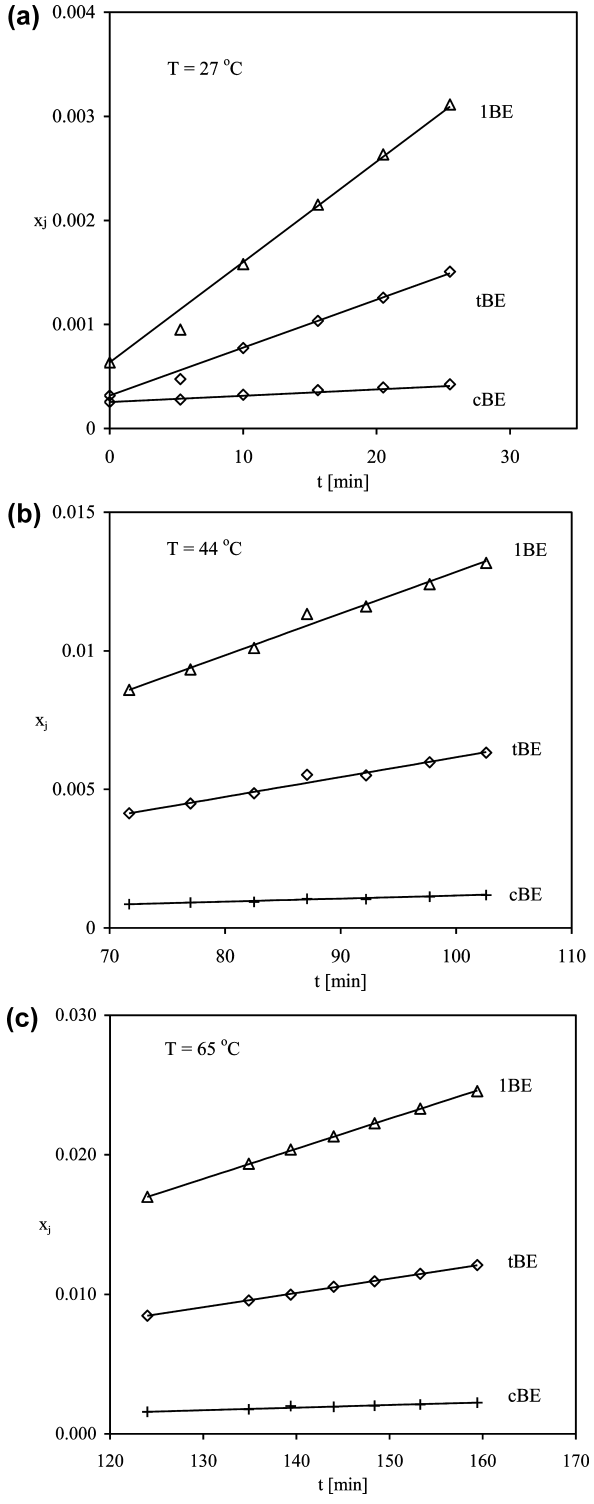

Figure 9. (a) Comparison of experimental (symbols) and model results (continuous lines) for run 3 in Table 1 at 27 °C. (b) Comparison of experimental (symbols) and model results (continuous lines) for run 3 in Table 1 at 44 °C. (c) Comparison of experimental (symbols) and model results (continuous lines) for run 3 in Table 1 at 65 °C.

rather to the suitability of kinetic expressions to describe the effect of composition changes (i.e., the prevailing expressions 6 and 7, as discussed in section 5).

As regards the modal values of E_i for reactions 1−9 (Figure 2), Boitiaux et al.[8] pointed out that over a Pd catalyst all reactions showed similar values, around 37500−42000 J/mol. Except E_4^I and E_9, the remaining values in Table 3, lie in the range 37500−46000 J/mol, showing a good agreement with the conclusions of Boitiaux et al.[8] It should be mentioned that these authors did not consider the isomerization between cBE and tBE, and no other background information was found for E_9. The value estimated for E_4^I is low, although it is recalled that the global kinetic coefficient for 1BE hydrogenation is a combination of k_4^I and k_4^{II} (see expression for r_4 in eq 7). When the activation energy is estimated for the latter, from relation 1, the value E_4^{II} = 67000 J/mol arises. Therefore, the actual effect of temperature on 1BE hydrogenation would correspond to an effective value larger than E_4^I (lying between 21000 and 67000 J/mol).

The set of values for the kinetic parameters in Tables 2 and 3 were used to simulate the results from runs 6 and 7 (Table 1), which were not involved in parameter estimation. The main feature of this pair of experiments is that they were carried out at the extreme values of the temperature range of interest (26 and 64 °C). In this regard, it should be noted that values of the ratios between adsorption constants K_{BD}/K_{1BE}, K_{cB}/K_{1BE}, and K_{tBE}/K_{1BE} taken at 44 °C (Table 2) were used in model calculations. The comparison with the model results is presented in Figures 10 and 11. An excellent agreement is found for run 6 that was performed at the upper extreme of the temperature range (64 °C) with an initially high concentration of 1BE. The good predictions of the decay of x_{BD}, the inhibition of 1BE reactions, and the distribution of products in the first part of the run are to be remarked. Also, at longer reaction times, when H_2 is in excess, the consumption of 1BE, the distribution of isomers, and BA formation are very well simulated. A good agreement in all respects is also found for run 7 (at the lowest temperature of 26 °C) in Figure 11, although simulation of 1BE isomerization seems to be somewhat slower than the actual rate, in the range 100−150 min.

Some comments are due as regards the dependence of the adsorption equilibrium ratios on temperature. By far, the most relevant ratios are those between the adsorption constants of each impurity (BY and BD) and the adsorption constant of each olefin. An inspection of the values of the ratios in Table 2 easily reveals that the largest of these relevant ratios is K_{BD}/K_{1BE}, which presents a modal value of 1700. This value stresses the excellent intrinsic selectivity of the catalyst for BD and BY hydrogenation reactions. At the same time, the estimation of such a large value has been uncertain (large confidence interval, Table 2) with our current experimental facilities.[12] A more sensitive instrumentation is necessary to measure with precision the very low concentration of BD at which 1BE can compete for adsorption sites and a more frequent sampling from the reacting mixture will also be required, because of the fast BD hydrogenation at such low concentrations. It can be easily realized that the evaluation of the effect of temperature on K_{BD}/K_{1BE} would be even more uncertain within the relatively short temperature range (25−65 °C). Nonetheless, from a practical point of view, it can be checked by simulation that even a drop of K_{BD}/K_{1BE} by a factor of 3 would make no essential difference in the observed selectivity of the process. The good agreement shown by run 6 at 64 °C with the simulation using K_{BD}/K_{1BE} at 44 °C (Figure 10) experimentally supports this concept, as K_{BD}/K_{1BE} should decrease with temperature (the heat of adsorption of BD is definitely larger than that of 1BE, e.g. Coq and Figueras[5]).

dx.doi.org/10.1021/ie3029027 | Ind. Eng. Chem. Res. 2013, 52, 5849−5861

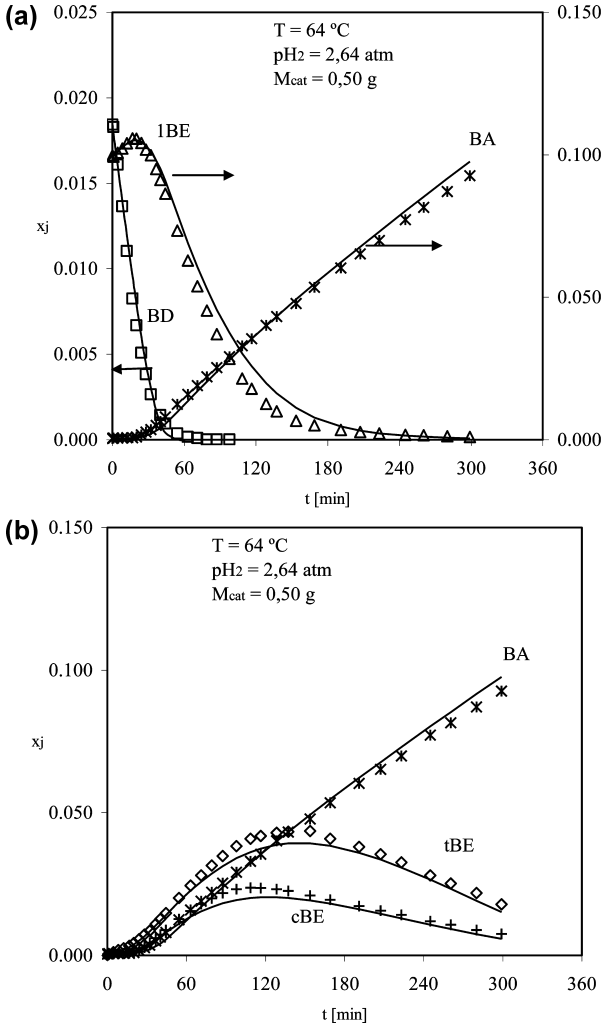

Figure 10. (a) Comparison of experimental (symbols) and model results (continuous lines) for run 6 in Table 1. BD, 1BE, and BA mole fractions vs reaction time. (b) Comparison of experimental (symbols) and model results (continuous lines) for run 6 in Table 1. BA, cBE, and tBE mole fractions vs reaction time.

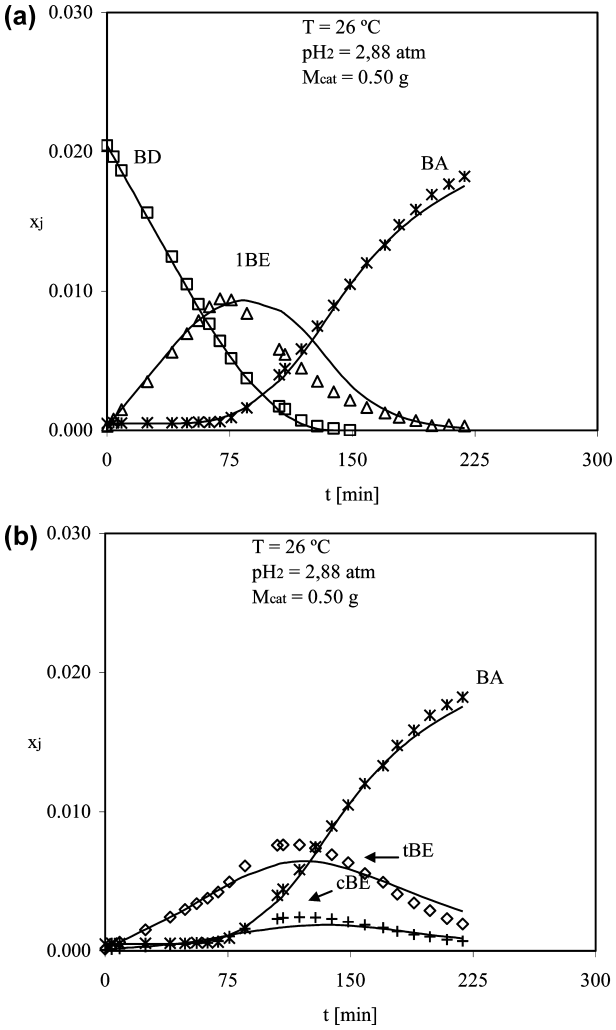

Figure 11. (a) Comparison of experimental (symbols) and model results (continuous lines) for run 7 in Table 1. BD, 1BE, and BA mole fractions vs reaction time. (b) Comparison of experimental (symbols) and model results (continuous lines) for run 7 in Table 1. BA, cBE, and tBE mole fractions vs reaction time.

As regards the ratio of adsorption constants between the *n*-butenes, the values K_{cBE}/K_{1BE} and K_{tBE}/K_{1BE} at 44 °C (Table 2) do not depart much from unity. The simultaneous occurrence of all hydrogenation and isomerization reactions involving the *n*-butenes (i.e., reactions 4−9 in Figure 2) makes difficult the estimation of such adsorption constant ratios, and therefore, a relatively large confidence interval arose (Table 2). It cannot be expected, however, that temperature exerts a significant effect upon them, as their interaction with the active sites is most probably similar and so should be their adsorption heats. Actually, if differences in entropic effects are ignored, the value K_{tBE}/K_{1BE} = 0.27 at 44 °C corresponds to a difference of only 3440 J/mol in the heats of absorption of tBE and 1BE. The good agreement between simulation and independent experiments at 26 and 64 °C (Figures 10 and 11) indicates that keeping the ratios K_{cBE}/K_{1BE} and K_{tBE}/K_{1BE} at 44 °C does not introduce significant differences for predicting purposes.

Finally, the ratio K_{BD}/K_{BY} estimated in this work at 44 °C (Table 2) has been estimated with a reasonably good confidence interval (±13%), by virtue of the fact that only two competitive reactions occur simultaneously (BY and BD hydrogenation reactions) in the suitable composition range for its identification. Considering that the ratio of adsorption constants is very close to 1, K_{BY}/K_{BD} =1.18, it is difficult to envisage a large difference in the heats of adsorption of BD and BY (excluding the second adsorption step of BY, step d in the mechanism of Figure 4). In any case, the only practical implication of a moderate change of K_{BD}/K_{BY} (say, by a factor of 2) within the significant temperature range will be a very slight variation in the total time needed to extinguish both impurities.

It can be concluded at a high level of probability that evaluating adsorption constant ratios at 44 °C is adequate for modeling the process of selective hydrogenation of mixtures of BY and BD in *n*-olefin cuts within the relatively short temperature range of 25−65 °C.

8. CONCLUSIONS

The general purpose of this work was to present a set of values for the parameters characterizing a general kinetic model of the liquid-phase hydrogenation of small amounts of BY and BD in *n*-butene-rich streams on a commercial egg-shell catalyst with

dx.doi.org/10.1021/ie3029027 | Ind. Eng. Chem. Res. 2013, 52, 5849−5861

Pd as the main catalytic agent, in the temperature range of 25−65 °C.

The kinetic model is based on a proposed mechanism of elementary steps, which gives rise to expressions for the rates of 10 global reactions capable of representing the behavior of the system, as hydrogenation and isomerization (among the *n*-butenes) reactions proceed in time (in a batch reacting system) or, equivalently, along the catalyst bed in a continuous operation.

The undertaken task described in this contribution stems from two previous works. In Alves et al.,[10] the hydrogenation of BY was studied and modeled kinetically in the range $T = 27-62$ °C, almost independently of the occurrence of other reactions, a fact that was possible because BY is able to saturate the catalytic surface even at very low concentrations. On the other hand, Alves et al.[12] reported the results of experiments with initial mixtures of BD and all *n*-butenes (1BE, cBE and tBE) at different H_2 partial pressures, allowing the kinetic characterization of all significant reactions (reactions 1−9 in Figure 2) at a fixed temperature of 44 °C. On this basis, in the present contribution experiments were described and analyzed in order to fulfill the following specific goals:

(a) Assembling a global mechanism and the corresponding set of kinetic expressions for systems presenting both impurities BY and BD simultaneously. New experiments at 44 °C were used to this end. It has been shown that adding the elementary steps proposed previously[10,12] allows representing the competition of both species for the active sites and consequent hydrogenation. Thus, by fitting only the ratio of the adsorption constants K_{BY}/K_{BD} and using the values of the remaining kinetic parameters estimated individually,[10,12] it was possible to obtain a satisfactory match between experimental data and model results.

(b) Estimating the activation energies E_i of the kinetic coefficients k_i ($i = 1-9$) in the rate expressions of Figure 5 (E_{10} was reported in a previous contribution[10]). Three experimental runs employing high initial concentrations of BD, 1BE, and cBE, respectively, were performed and analyzed to this end. The modal values of E_i compared reasonably well with background information, and their confidence intervals were acceptably narrow.

(c) Testing the overall performance of the kinetic model and the set of estimated parameters on independent experiments. The results of two runs carried out until almost complete depletion of all unsaturated species and at the extremes of the temperature range studied (25−65 °C) were compared satisfactorily with model predictions (the runs were not involved in parameter estimation).

Kinetic expressions for the set of reactions in Figure 2 are displayed in Figure 5, and the whole set of estimated parameters are reported in Table 2 (at 44 °C) and Table 3 (activation energies and adsorption heat for the adsorption constant K_η). In turn, eqs 1 are the necessary relationships to evaluate dependent parameters. Finally, eq 2a expresses some of the H_2 inhibition terms (Table 2) that were not found as being statistically significant, and eq 2b shows that the catalytic surface remains fully covered by adsorbed species, if any unsaturated species remains in the liquid phase.

At present, the ratios between adsorption constants have been evaluated only at 44 °C. It has been discussed that the effect of temperature on those ratios in the range of about 25−65 °C can be expected to be mild. The good matching from predictions and independent experiments (point c quoted above) is in line with this assertion.

It is concluded that the sets of expressions and kinetic parameters presented in this contribution can be adopted as a reliable starting point to analyze and simulate the behavior of industrial reactors for selective hydrogenation of BY and BD in olefin-rich C4 cuts. Since the reported kinetic parameters correspond to the specific catalyst studied in the state of maximum activity, i.e. with a fresh catalyst loaded, an activity factor should be introduced to account for other commercial catalysts or for taking into account catalyst aging. In this respect, it is useful to recall the conclusion reached in Alves et al.[12] when testing several commercial catalysts: they show a very similar behavior, and the set of rate expressions given in Figure 5 most likely holds for all of them. The global strategy adopted for parameter fitting, as arising from this and our previous reports,[10,12] is also thought to provide a useful guideline if the kinetic model is to be tuned for different catalysts.

AUTHOR INFORMATION

Corresponding Author

*Tel.: 54-221-4210711. E-mail: jalves@quimica.unlp.edu.ar.

Notes

The authors declare no competing financial interest.

ACKNOWLEDGMENTS

We thank the financial support provided by Universidad Nacional de La Plata (UNLP) (PID 11/I136), by ANPCyT (PICT'05 14/38336), and by CONICET (PIP 0304). J.A.A., O.M.M., and G.F.B. are members of CONICET, and S.P.B. is a member of CIC-PBA.

REFERENCES

(1) Derrien, M. L. Selective Hydrogenation Applied to the Refining of Petrochemical Raw Materials Produced by Steam Cracking. *Stud. Surf. Sci. Catal.* **1986**, *27*, 613−666.

(2) Bond, G. C.; Webb, G.; Wells, P. B.; Winterbottom, J. M. Patterns of Behavior in Catalysis by Metals. *J. Catal.* **1962**, *1*, 74−84.

(3) Boitiaux, J. P.; Cosyns, J.; Robert, E. Liquid Phase Hydrogenation of Unsaturated Hydrocarbons on Palladium, Platinum and Rhodium Catalysts. Part I: Kinetic Study of 1-Butene, 1,3-Butadiene and 1-Butyne Hydrogenation on Platinum. *Appl. Catal.* **1987**, *32*, 145−168.

(4) Maetz, Ph.; Touroude, R. Modification of Surface Reactivity by Adsorbed Species on Supported Palladium and Platinum Catalysts During the Selective Hydrogenation of But-1-yne. *Appl. Catal., A* **1997**, *149*, 189−206.

(5) Coq, B.; Figueras, F. Bimetallic Palladium Catalysts: Influence of the Co-Metal on the Catalyst Performance. *J. Mol. Catal. A: Chem.* **2001**, *173*, 117−134.

(6) Molnár, A.; Sárkány, A.; Varga, M. Hydrogenation of Carbon-Carbon Multiple Bonds: Chemo-, Regio- and Stereo-Selectivity. *J. Mol. Catal. A: Chem.* **2001**, *173*, 185−221.

(7) Schäfer, P.; Wuchter, N.; Gaube, J. Kinetic Studies on the Hydrogenation of 1,3 Butadiene, 1-Butyne and their Mixtures. *Stud. Surf. Sci. Catal.* **2000**, *130*, 2051−2056.

(8) Boitiaux, J. P.; Cosyns, J.; Derrien, M.; Leger, G. Proper Design of Butadiene Selective Hydrogenation Process for Maximum 1-Butene Yield by Using Comprehensive Kinetic Modeling. *AIChE Spring Natl. Meet., Conf. Proc.* **1985**, Paper No. 1453.

(9) Seth, D.; Sarkar, A.; Ng, F. T. T.; Rempel, G. L. Selective Hydrogenation of 1,3-Butadiene in Mixture with Isobutene on a Pd/Alumina Catalyst in a Semi-Batch Reactor. *Chem. Eng. Sci.* **2007**, *62*, 4544−4557.

(10) Alves, J. A.; Bressa, S. P.; Martínez, O. M.; Barreto, G. F. Kinetic Study of the Liquid-Phase Selective Hydrogenation of 1-Butyne in Presence of 1-Butene over a Commercial Palladium-Based Catalyst. *Chem. Eng. Res. Des.* **2011**, *89*, 384−397.
(11) Alves, J. A.; Bressa, S. P.; Martínez, O. M.; Barreto, G. F. Kinetic Study of the Liquid-Phase Hydrogenation of 1-Butyne over a Commercial Palladium/Alumina Catalyst. *Chem. Eng. J.* **2007**, *125*, 131−138.
(12) Alves, J. A.; Bressa, S. P.; Martínez, O. M.; Barreto, G. F. Kinetic Study of the Selective Catalytic Hydrogenation of 1,3-Butadiene in a Mixture of n-Butenes. *J. Ind. Eng. Chem.* **2012**, *18*, 1353−1365.
(13) Ardiaca, N. O.; Bressa, S. P.; Alves, J. A.; Martínez, O. M.; Barreto, G. F. The Case of Liquid-Phase Hydrogenation of 1,3-Butadiene and n-Butenes on Commercial Pd Catalysts. *Catal. Today* **2001**, *64*, 205−215.
(14) Bressa, S. P.; Martínez, O. M.; Barreto, G. F. Kinetic Study of the Hydrogenation and Hydroisomerization of the n-Butenes on a Commercial Palladium/Alumina Catalyst. *Ind. Eng. Chem. Res.* **2003**, *42*, 2081−2092.
(15) Ardiaca, N. O.; Bressa, S. P.; Alves, J. A.; Martinez, O. M.; Barreto, G. F. Kinetic Study of the Liquid Phase Hydrogenation of 1,3-Butadiene and n-Butenes on a Commercial Pd/Al_2O_3 Catalyst. *Stud. Surf. Sci. Catal.* **2001**, *133*, 527−534.
(16) White, C. W. Butadiene Production Process Overview. *Chem.-Biol. Interact.* **2007**, *166*, 10−14.
(17) Nijhuis, T. A.; Dautzenberg, F. M.; Moulijn, J. A. Modeling of Monolithic and Trickle-Bed Reactors for the Hydrogenation of Styrene. *Chem. Eng. Sci.*. **2003**, *58*, 1113−1124.
(18) Alves, J. A. Cinética de la Hidrogenación Catalítica Selectiva de 1-Butino y 1,3-Butadieno en Presencia de n-Butenos (Kinetics of Selective Catalytic Hydrogenation of 1-Butyne, 1,3-Butadiene in the Presence of N-Butenes [Engl. Transl.]). Ph.D. Thesis. Universidad Nacional de La Plata: La Plata, Argentina, 2009.
(19) Goetz, J.; Yu Murzin, D.; Touroude, R. Kinetic Aspect of Selectivity and Stereoselectivity for Buta-1,3-diene Hydrogenation over a Palladium Catalyst. *Ind. Eng. Chem. Res.* **1996**, *35*, 703−711.
(20) Boudart, M.; Hwang, H. S. Solubility of Hydrogen in Small Particles of Palladium. *J. Catal.* **1975**, *39*, 44.
(21) Decker, S.; Frennet, A. Thermodynamic Parameter of H_2 Adsorption Criteria to Characterize Silica-Supported Palladium Catalyst. *Catal. Lett.* **1997**, *46*, 145.
(22) Stewart, W. E.; Caracotsios, M.; Sørensen, J. P. Parameter Estimation from Multiresponse Data. *AIChE J.* **1992**, *38*, 641−650.
(23) Bressa, S. P.; Mariani, N. J.; Ardiaca, N. O.; Mazza, G. D.; Martínez, O. M.; Barreto, G. F. An Algorithm for Evaluating Reaction Rates of Catalytic Reaction Networks With Strong Diffusion Limitations. *Comput. Chem. Eng.* **2001**, *25*, 1185−1198.
(24) Box, G. E. P. Fitting Empirical Data. *Ann. N. Y. Acad. Sci.* **1960**, *86*, 792−816.